



# In-situ methane enrichment in continuous anaerobic digestion of pig slurry by zero-valent iron nanoparticles addition under mesophilic and thermophilic conditions

Míriam Cerrillo <sup>a</sup>, Laura Burgos <sup>a</sup>, Beatriz Ruiz <sup>a</sup>, Raquel Barrena <sup>b</sup>, Javier Moral-Vico <sup>b</sup>, Xavier Font <sup>b</sup>, Antoni Sánchez <sup>b</sup>, August Bonmatí <sup>a,\*</sup>

<sup>a</sup> IRTA. GIRO. Torre Marimon. E-08140, Caldes de Montbui, Barcelona, Spain

<sup>b</sup> GICOM, Department of Chemical, Biological and Environmental Engineering, Universitat Autònoma de Barcelona, Edifici Q, 08193 Cerdanyola del Vallès, Barcelona, Spain

## ARTICLE INFO

### Article history:

Received 5 May 2021

Received in revised form

2 August 2021

Accepted 19 August 2021

Available online 27 August 2021

### Keywords:

Anaerobic digestion

Nanoparticles

Methane

Iron zero-valent

Pig slurry

Biogas upgrading

## ABSTRACT

The effect of zero-valent iron nanoparticles (nZVI) addition on methane production during anaerobic digestion of pig slurry was assessed. Experiments were conducted using two experimental set-ups: batch and long-term continuous operation at a fixed nZVI dosage. Two different temperature operation ranges (mesophilic and thermophilic) were assessed. Biogas production and methane content were monitored, and the specific methanogenic activity of the biomass and nZVI oxidation state were evaluated at different times. The results of batch experiments at mesophilic temperature operation showed an inhibition of methane production at all tested dosages (42, 84, 168 and 254 mg<sub>nZVI</sub> g<sup>-1</sup> VSS concentrations), while methane production was boosted with the lowest dosage in thermophilic temperature operation. In continuous operation, nZVI addition produced an increase in methane content of biogas, achieving values between 80 and 85% in both temperature ranges. The average methane production rate increased 165% and 94% with respect to the control in thermophilic and mesophilic temperature range, respectively. The oxidation state of nZVI showed a value of +3 almost immediately after contact with substrate and a slower progressive oxidation during the reactors operation. The obtained results indicate that nZVI addition in anaerobic digestion is an interesting strategy for in situ biogas upgrading.

© 2021 Elsevier Ltd. All rights reserved.

## 1. Introduction

Biogas is a biofuel obtained from anaerobic digestion with multiple uses since it can be directly burnt for thermal energy production or power generation. Biogas is mainly composed of methane (50–70%) and CO<sub>2</sub> (30–50%), and can be upgraded to natural gas grade to be suitable for other uses such as transport fuel and injection in natural gas grid [1]. Various energy demanding physical and chemical methods are used nowadays for biogas upgrading, based on CO<sub>2</sub> and CH<sub>4</sub> separation from the biogas stream, such as scrubbing, pressure swing adsorption (PSA) or membrane separation [2]. Alternatively, other technologies under development are based on the conversion of CO<sub>2</sub> to CH<sub>4</sub>, such as the electromethanogenesis process that can take place in

bioelectrochemical system (BES) [3].

The enhancement of methane production in anaerobic digestion is subject of constant research, and several technologies and techniques can be applied, such as bioaugmentation or co-digestion [4]. The application of nanoparticles (NPs) is receiving increasing attention as an approach to increase methane production in anaerobic digestion. NPs have been reported to be useful for wastewater treatment applications [5]. NPs could act as electron donors or acceptors and cofactor of important enzymes in various bioprocesses, which will enhance their yields [6]. The effect of different metallic nanoparticles on biogas production in anaerobic digestion has been studied, such as silver NPs on sewage sludge anaerobic digestion [7]; iron oxide (Fe<sub>2</sub>O<sub>3</sub>) and titanium dioxide (TiO<sub>2</sub>) NPs on cattle manure anaerobic digestion [8]; iron oxide (Fe<sub>2</sub>O<sub>3</sub>) NP on two-stage anaerobic digestion with waste sludge [9]; TiO<sub>2</sub> NPs, on anaerobic digestion of lignocellulosic substrate [10]; magnetite and iron zero-valent, on anaerobic digestion of sludge [11]; magnetite on chicken litter anaerobic digestion [12]; or iron

\* Corresponding author.

E-mail address: [august.bonmati@irta.cat](mailto:august.bonmati@irta.cat) (A. Bonmati).

zero-valent, on anaerobic granular sludge [13]. Some studies have reported an inhibitory effect of NPs, which will produce toxic effects over microorganisms, generally dosage and specific NPs dependant [14]. A previous study with nano zero-valent iron (nZVI) has reported inhibition of methanogenesis due to its disruption of cell integrity [15]. On the contrary, no ecotoxicity has been detected in other studies [16], or an increase in methane production has been reported when iron NPs were added [13,17,18]. Several comprehensive reviews report the impacts of different kinds of nanoparticles on anaerobic digestion processes [6,19,20].

The use of nZVI in anaerobic digestion has been proposed as a biogas upgrading method, since it may improve the proportion of methane to the detriment of CO<sub>2</sub> [2]. This technique could be applied with a low investment cost and a minimum process complexity since it will not consist of CO<sub>2</sub> removal or adsorption (i.e. zeolites) phases, but direct CO<sub>2</sub> conversion into methane. In addition to biogas methane enrichment, it has been reported that biogas production is also enhanced by nZVI addition [21]. The impact of different nZVI concentrations on microbial growth has been also assessed, reporting that different conditions of substrate composition, pH or temperature produced changes in organic matter removal efficiencies [22]. Although the increasing amount of published research on the impacts of NPs on anaerobic digestion, most of the nZVI studies focus on batch and short term assays, and waste activated sludge usage. Only a few studies use high strength wastewater such as livestock manure as a substrate [21,23–25]. Short term batch investigations have reported an enhancement in methane production [26–29], while some longer term investigations showed an increase of methane production in the early stages of experiments, which is followed by an inhibition phase [30]. A methane production increase depending on NP dosage was reported in other studies [31,32].

To the extent of our knowledge, this study is the first to examine the effects of nZVI dosage onto anaerobic digestion of pig slurry on long term and continuously fed assays, and to compare mesophilic and thermophilic operation temperature conditions.

Additionally, although the effect of iron nanoparticles on anaerobic digestion has been previously reported, most of the published literature does not include much information about the behaviour of iron. In this work, the morphological and microstructural study of nZVI is presented. Furthermore, a novel study on the evolution of the oxidation state of this material when added to the anaerobic medium has been performed.

The aim of this study was to evaluate the impact of nZVI on methane production during anaerobic digestion of pig slurry, both under mesophilic and thermophilic temperature conditions, and in batch and continuous operation. Methanogenic activity tests have been applied to assess the change of microbial biomass after NPs addition. Furthermore, Scanning Electron Microscope (SEM) and Electron energy-loss spectroscopy in a transmission electron microscope (TEM-EELS) have been used to monitor the morphology, microstructure and oxidation state of the NPs.

## 2. Materials and methods

### 2.1. Nanoparticles and feeding substrate

nZVI NPs were synthesized adding a sodium borohydride (NaBH<sub>4</sub>, ≥98%, Sigma-Aldrich) aqueous solution to a ferrous chloride (III) (FeCl<sub>3</sub>, ≥98%, Sigma-Aldrich) aqueous solution, using Milli-Q grade water, based on the methodology described elsewhere [33]. Briefly, for batch assays, 200 mL of 3.72 M sodium borohydride was added dropwise to 200 mL of 0.93 M ferrous chloride while the solution was vigorously stirred under a N<sub>2</sub> stream at room

temperature. The obtained nZVI was rinsed with Milli-Q grade water and purged with nitrogen gas. The final concentration of nZVI in the stock solution was 0.47 M.

For continuous assays, to reduce the volume of stock solution added to the reactors in each pulse, the concentration of the nZVI solution was increased. A 0.93 M concentrated nZVI stock solution was prepared, mixing 75 mL of 7.45 M sodium borohydride and 75 mL of 1.86 M ferrous chloride with the same methodology described for batch nZVI solution.

The pig slurry used as feeding was collected at Puigllong farm (Gurb, Barcelona, Spain), sieved (500 μm) and frozen (−20 °C) up to its use, to assure stable composition during all the experiment.

### 2.2. Batch assays at different nZVI dosage

Batch experiments (biochemical methane potential tests) were conducted to investigate the effect of different concentrations of nZVI on the production of methane in pig slurry anaerobic digestion. 120 mL serum bottles were used for this purpose, and each condition was prepared in triplicate. These serum bottles were filled with a 50 g solution composed of the inoculum (4 g<sub>VSS</sub> L<sup>−1</sup>), pig slurry as substrate (4 g<sub>COD</sub> L<sup>−1</sup>) and the different concentrations of NPs (0, 42, 84, 168 and 254 mg<sub>NP</sub> g<sup>−1</sup> VSS). These doses were based on previous assays performed by the authors in semi-continuous anaerobic digestion tests of sewage sludge, which had proven to be effective for methane production increase [34]. The digested sludge from a mesophilic and a thermophilic lab-scale anaerobic digesters were used as inoculums to test both operational temperature ranges. A control in triplicate, without pig slurry substrate, was included in the setup. The bottles were sealed with rubber stoppers and capped with aluminium crimp caps. The headspace was purged with N<sub>2</sub> for 5 min in order to remove O<sub>2</sub> and assure anaerobic conditions. The bottles were incubated for 40 days at 37 ± 2 °C and 55 ± 2 °C for mesophilic and thermophilic temperature ranges, respectively. Methane production was monitored periodically by taking a gas sample (0.2 mL) from the headspace with a syringe and analysing the gas composition by gas chromatography.

Biogas was accumulated in the serum bottles headspace until the end of the assay. Pressure monitoring indicated that there was no high overpressure, so microorganisms were not affected, and it was not necessary to empty the headspace. The cumulative methane yield (V<sub>CH<sub>4</sub></sub>, mL) of each serum bottle was calculated using the N<sub>2</sub> concentration, which should be constant throughout the assay, to correct the molar fractions as follows (Equation (1)):

$$V_{CH_4} = V_h \frac{X_{N_2}^0 \cdot X_{CH_4}}{1 - X_{CH_4} - X_{CO_2}} \quad (1)$$

where V<sub>h</sub> is the headspace volume (mL) of the serum bottle, X<sub>N<sub>2</sub></sub><sup>0</sup> is the molar fraction of nitrogen measured at the beginning of the assay, and X<sub>CH<sub>4</sub></sub> and X<sub>CO<sub>2</sub></sub> are the molar fractions of CH<sub>4</sub> and CO<sub>2</sub>, respectively, present in biogas determined by gas chromatography.

Pressure build-up along the assay was calculated by the increase in the number of moles determined by gas chromatography and the ideal gas equation (Equation (2)).

$$PV = nRT \quad (2)$$

where P is pressure (atm), V is the serum bottle headspace volume (L), n is the number of mole of gas determined by gas chromatography (N<sub>2</sub>, CH<sub>4</sub> and CO<sub>2</sub>), R is ideal gas constant (0.082 atm L mol<sup>−1</sup> K<sup>−1</sup>), and T is temperature (K).

### 2.3. Continuous experimental set-up

Three lab-scale continuous stirred tank reactors (CSTR) were used for the experiments. Two of them were operated in mesophilic temperature range (36 °C), and the third one was operated at thermophilic temperature range (55 °C). The anaerobic digesters (AD) consisted of a cylindrical glass reactor (25 cm diameter, volume of 5 L) fitted with a heat jacket with hot water circulating to keep the temperature at the desired value. A temperature probe was placed into the reactor lid for temperature monitoring. Continuous mixing was supplied to each reactor using an overhead stirrer. Biogas production was measured with a gas counter ( $\mu$ Flow, Bioprocess Control AB, Sweden). All the digesters were already in operation, fed with pig slurry for more than a year.

### 2.4. Reactors operation

The three ADs were fed in a continuous mode with raw pig slurry with a hydraulic retention time (HRT) of 10 days for the thermophilic AD and 20 days for the mesophilic ADs. The pig slurry was diluted with tap water to obtain the desired organic load. The main characteristics of the diluted pig slurry were as follows: total solids (TS),  $29 \pm 4 \text{ g kg}^{-1}$ ; volatile solids (VS),  $19 \pm 3 \text{ g kg}^{-1}$ ; total chemical oxygen demand (TCOD),  $36 \pm 5 \text{ g kg}^{-1}$ ; total Kjeldahl nitrogen (TKN),  $2.4 \pm 0.5 \text{ g kg}^{-1}$ ; ammonia nitrogen,  $1.7 \pm 0.5 \text{ g kg}^{-1}$ . The reactors were operated during 265 days in 3 different phases (Table 1), with an organic loading rate (OLR) of  $1.7 \pm 0.4 \text{ kg}_{\text{COD}} \text{ m}^{-3} \text{ day}^{-1}$  and  $4.1 \pm 1.1 \text{ kg}_{\text{COD}} \text{ m}^{-3} \text{ day}^{-1}$  in mesophilic and thermophilic reactors, respectively.

In Phase 1, one of the mesophilic ADs was used as control (MC), while a weekly nZVI pulse of  $84 \text{ mg g}^{-1}$  SSV was injected in the second mesophilic reactor (M). In turn, the thermophilic (T) reactor received a nZVI weekly pulse of  $42 \text{ mg g}^{-1}$  SSV. The dosages were chosen according to the results obtained in the batch assays performed, as will be described in Section 3.1. The addition of nZVI corresponding to a week was added in a unique pulse. In order to compare the results of the thermophilic reactor with a control, a previous 63-day period of the same reactor before starting nZVI addition was considered as Phase 0.

In Phase 2, a weekly pulse of nZVI was injected in the MC reactor, in the same conditions as it was applied in the M reactor in Phase 1. In the case of the T and M reactors, the dosages applied in Phase 2 were equal to those applied in Phase 1 but divided into 2 injections per week.

Finally, in Phase 3, NPs addition was stopped in all reactors, to determine if NPs effects on biogas production and its composition (richness of  $\text{CH}_4$  and  $\text{CO}_2$ ) were long lasting.

Each phase was maintained at least for 3 HRT to ensure a stable operation. For each experimental condition, methane production rate ( $\text{L}_{\text{CH}_4} \text{ kg}_{\text{VS}}^{-1} \text{ d}^{-1}$ ) and chemical oxygen demand (COD) removal efficiency were used as control parameters, by taking weekly samples. Biogas composition was analysed on weekdays, to better

**Table 1**  
Operation phases of the mesophilic control (CM), mesophilic (M) and thermophilic reactors (T).

| Phase | Period (d) | Frequency of nZVI injection (times/week) |   |   | nZVI concentration of the pulse ( $\text{mg}_{\text{NP}} \text{ g}^{-1} \text{ SSV}_{\text{added}}$ ) |    |    |
|-------|------------|--|---|---|---|----|----|
|       |            | CM                                       | M | T | CM  | M  | T  |
| 0     | 63         | –  | – | 0 | –   | –  | –  |
| 1     | 125        | 0  | 1 | 1 | –   | 84 | 42 |
| 2     | 70         | 1  | 2 | 2 | 84  | 42 | 21 |
| 3     | 70         | 0  | 0 | 0 | –   | –  | –  |

understand the effect of nZVI addition on the anaerobic digestion process.

### 2.5. Specific methanogenic activities

To determine the changes in metabolic pathways when nZVI was applied, sludge samples were collected from each reactor at the end of Phase 1 and 2, and also at the end of Phase 0 in the thermophilic reactor, to perform specific methanogenic activity tests (SMA). Tests were carried out using 120 mL serum bottles, following the methodology described elsewhere [35]. A volatile fatty acid (VFA) mix (acetate/propionate/butyrate, 70/20/10), acetate, and  $\text{H}_2$  were used as substrates. The serum bottles were filled with a 50 mL solution of the mesophilic or thermophilic sludge ( $1.5 \text{ g}_{\text{VSS}} \text{ L}^{-1}$ ), substrate ( $5 \text{ g}_{\text{COD}} \text{ L}^{-1}$ ), macronutrients, micronutrients and bicarbonate ( $1 \text{ g NaHCO}_3 \text{ g}_{\text{COD added}}^{-1}$ ). A control duplicate without the medium was included in the set-up. The bottles were sealed with rubber stoppers and capped with aluminium crimp caps. The headspace was purged for 5 min with  $\text{N}_2$  in order to assure anaerobic conditions.  $\text{H}_2$  substrate addition was performed by injection of 60 mL of high purity  $\text{H}_2$  gas ( $\geq 99.999\%$ ) through the septum once the serum bottle was sealed and purged. The bottles were incubated for 60 days at  $37 \pm 2 \text{ }^\circ\text{C}$  and  $55 \pm 2 \text{ }^\circ\text{C}$  for mesophilic and thermophilic temperature ranges, respectively. Methane production was monitored periodically by taking a gas sample (0.2 mL) from the head space with a gas-tight syringe and analysing the gas composition by gas chromatography. Biogas was accumulated in the serum bottles headspace until the end of the assay, and  $\text{CH}_4$  volume and pressure build-up were calculated as described in Equations (1) and (2).

The SMA was calculated from the linear increase in the  $\text{CH}_4$  concentration at the beginning of the experiments (when no lag phase was observed) divided by the amount of VSS.

### 2.6. Analytical methods and calculations

Chemical oxygen demand (COD), ammonium nitrogen ( $\text{NH}_4^+\text{-N}$ ), Kjeldahl nitrogen (TKN), total and volatile solids (TS, VS), total suspended and volatile suspended solids (TSS, VSS), pH, total and partial alkalinity were determined according to Standard Methods 5220 [36]. Partial alkalinity (PA), which corresponds roughly to bicarbonate alkalinity, was determined by titration with  $\text{H}_2\text{SO}_4$  from the original pH sample to pH 5.75. Total alkalinity (TA, titration to pH 4.3) corresponds to VFA alkalinity added to bicarbonate alkalinity [37]. The bulk solution pH in each sample was measured using a CRISON 2000 pH electrode.  $\text{NH}_4^+\text{-N}$  and TKN were analysed by a Büchi KjelFlex K-360 distiller, and a Metrohm 702 SM autotitrator. Volatile fatty acids (VFA) were quantified by gas chromatography using a VARIAN CP-3800 (Varian, USA) chromatograph equipped with a flame ionisation detector (FID). Methane content in biogas was determined using a VARIAN CP-3800 (Varian, USA) gas chromatograph equipped with a Hayesep® Q packed column (matrix 80/100) and a thermal conductivity detector (TCD). A sample of 200  $\mu\text{L}$ , which was taken from the headspace of serum bottles (batch and SMA tests) or reactors (continuous assays) through the septum, was manually injected by means of a gas tight syringe (500  $\mu\text{L}$  Hamilton Sampleblock Syringe) at a temperature of  $180 \text{ }^\circ\text{C}$ . The carrier gas was helium, with a flux of  $40 \text{ mL min}^{-1}$ . The oven and detector temperatures were set at  $90$  and  $180 \text{ }^\circ\text{C}$ , respectively. Iron concentration of the effluent and of the reactor content was determined in Phase 3 of operation by inductively coupled plasma optical emission spectroscopy (ICP-OES) (Optima 4300DV, PerkinElmer).

Data were analysed using one-way analysis of variance (ANOVA). Whenever significant differences of means were found,

the Tukey test at the 5% significance level was performed for separation of means. Statistical analysis was performed using the R software package (R project for statistical computing, <http://www.r-project.org/>).

### 2.7. Nanoparticles characterization

Samples from the content of the reactors M and T were taken during Phase 1, on day 112–115 of operation (M reactor) and 176 to 179 (T reactor), to characterise nZVI structure and oxidation state after a pulse. Samples were also taken during Phase 3, in order to monitor the evolution of nZVI once the pulses were stopped, on days 226, 239 and 253 of operation (mesophilic reactors) and 290, 303 and 317 (thermophilic reactor).

The characterization of nZVI in terms of size, distribution and morphology was performed using a scanning electron microscope (SEM), with a Quanta FEI 200 FEG-ESEM instrument, equipped for analysis of Energy Dispersive X-ray (EDX). A FEI Tecnai G2 F20 HR(S)TEM equipped with a Gatan Image Filter (GIF) Quantum SE 963 @ 200 kV to obtain EELS spectra was also used to analyse the size, distribution and morphology of nZVI. Besides, selected areas electron diffraction images (SAED) was used to study the microstructure of the material with high resolution images. The utility for measuring the energy spectrum electron loss (EELS) was used to obtain information about the oxidation state of nZVI.

The EELS spectra defines a  $L_{32}$  ratio, which corresponds to a defined oxidation state of iron according to Tan et al. [38]. According to them, a value of 2.99 of this ratio corresponds to zerovalent iron, while oxidation states of +2 and +3 correspond to 3.99 and 4.55  $L_{32}$  values respectively. Two different types of tests were performed for comparison: test number 1 consisted in studying nZVI evolution in a batch test using a 25 mL hermetically closed and nitrogenized bottle. This test was performed with two combinations: test 1a) nZVI in an aqueous suspension up to 14 days, and test 1b) nZVI added to anaerobic inoculum + pig slurry (anaerobic medium) at the same concentration of continuous reactors up to 7 days. In test number 2, nZVI samples were collected from continuous reactors operated up to three days: test 2a) mesophilic reactors, and test 2b) thermophilic reactors.

## 3. Results and discussion

### 3.1. Methane production in batch assays at different nZVI dosage

Specific methane productions and initial slopes obtained in the batch assays under mesophilic and thermophilic conditions are presented in Fig. 1. For both temperature ranges, maximum specific methane productions were obtained with no NPs addition (267.6 and 235.0  $L_{CH_4} kg_{VSS}^{-1}$  for mesophilic and thermophilic operation, respectively). Under mesophilic conditions, increasing nZVI concentration decreased methane production. Differently, under thermophilic conditions, the concentrations of 0 and 42  $mg_{NP} g^{-1}$  VSS achieved similar methane production, with no significant statistical differences ( $p < 0.05$ ). Interestingly, all NPs concentrations boosted methane production during the first 20 days of the thermophilic batch assay, as it is shown by the initial slopes. Figure S1 shows the accumulated methane production of the different tested conditions. It is difficult to compare the obtained results with previous reports because of the different ways of expressing NPs dosage. Most studies report the dosage in terms of volume ( $mg L^{-1}$ ), when in other works it is preferred to express it as a function of the organic matter present in the substrate, as stated by Lizama and coworkers [39]. The nZVI concentrations tested in this assay were between 2.5 and 15.4 mM, and previous works have reported an inhibition of methanogenic activity with increasing

concentrations of nZVI in mesophilic glucose anaerobic digestion (in a range of 1–30 mM) [15]. Other work has reported an increase in specific biogas and methane production in cattle manure batch mesophilic anaerobic digestion when increasing nZVI concentrations from 5 to 20  $mg L^{-1}$  [21]. Batch assays with poultry litter and nZVI at 15, 50 and 100  $mg L^{-1}$  (1.68, 5.58 and 11.17  $mg_{NP} g^{-1}$  VS) increased methane production up to 29.1% compared to no nZVI addition [24]. Finally, adding 9  $mg_{NP} g^{-1}$  VS to sewage sludge mesophilic anaerobic batch assays increased biogas yield and methane content 135% and 186%, respectively, with respect to control [39]. The concentrations of those assays are also lower than the ones tested in this assay, which range from 140 to 860  $mg L^{-1}$ .

Wu and coworkers (2015) tested ZVI in batch anaerobic digestion of swine manure, although using powder form instead of NP, with concentrations as high as 50  $g L^{-1}$ . It was reported that although methane production increased with the applied dose, excessive ZVI doses did not stimulate methane production further and probably exerted negative effects on microbial activity [40]. The addition of 5  $g L^{-1}$  of ZVI powder to ammonia-rich swine manure batch anaerobic digestion was reported to achieve 54.2% higher methane yield relative to control [41].

This batch assay results show a clear inhibition of methane production in mesophilic temperature conditions and an initial methane boost in thermophilic conditions, which may be due to an excessive dosage compared to other works. Other possible inhibition causes in batch assays are discussed later in Section 3.2.4.

Regarding the different behaviour between mesophilic and thermophilic conditions, it has been reported previously an improvement in COD removal efficiency when increasing AD temperature from 37 °C to 50 °C with a 50  $g L^{-1}$  addition of nZVI (13.37% and 33.43%, respectively), while the control reactor reduced its activity with the increase of temperature [22]. Furthermore, in this study, the thermophilic inoculum used in batch assays was obtained from the thermophilic reactor used in continuous operation mode. This reactor had been operated in previous assays with high organic and nitrogen loading rates, and hydrogenotrophic methanogens represented a high proportion of methanogenic archaea [42]. Biomass may be better acclimated and able to shift to hydrogenotrophic methanogenic metabolic pathway compared to the mesophilic temperature reactor, as the results of the SMA test have also shown (Section 3.3).

Although batch assays results have not shown a clear improvement in methane production, previous assays of the group in semi-continuous operation mode had proven to increase methane production in AD of sewage sludge in the tested dose range [34]. Consequently, the doses chosen to be tested in continuous operation assay were in the low concentration range, 84 and 42  $mg_{NP} g^{-1}$  VSS<sub>added</sub> for mesophilic (M) and thermophilic (T) reactors, respectively, to test if inhibition could be avoided in continuous operation mode, and to be able to compare the results obtained in both operation modes. Furthermore, continuous operation mode could have an acclimation effect on the biomass that may result in different behaviour of the anaerobic digestion process compared to batch tests [34].

### 3.2. Methane production in continuous assays with nZVI addition

#### 3.2.1. Thermophilic temperature range operation

An increase in the content of methane in the biogas was produced with nZVI addition in continuous anaerobic digestion. As shown in Fig. 2a, the percentage of methane in the thermophilic reactor increased from 64% in Phase 0 to a maximum value of 87% in Phase 1. Methane content showed an increase after each weekly pulse of nZVI, which was maintained for several days, followed by a decrease, until a new pulse was added. The boost in methane

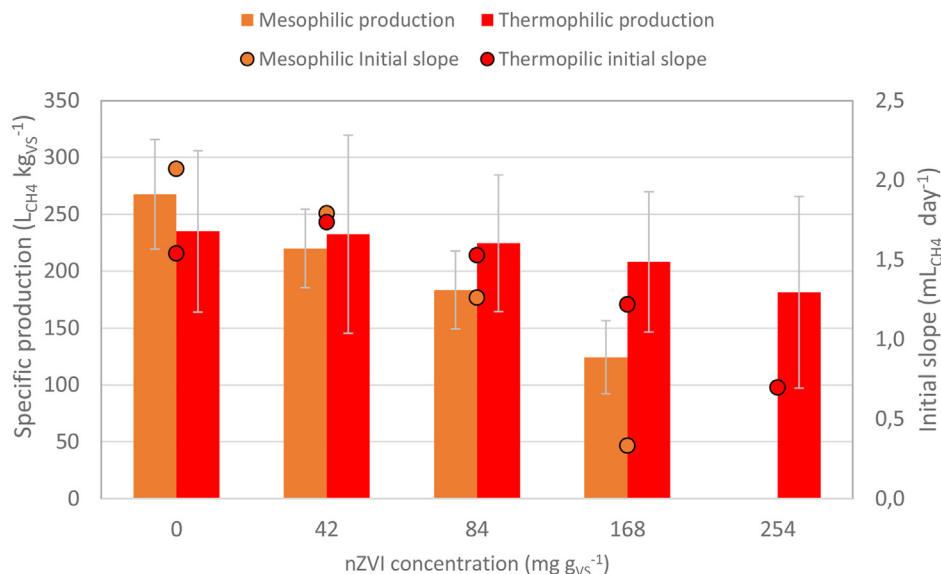


Fig. 1. Specific methane production and initial slope of the batch assays performed in mesophilic and thermophilic temperature conditions with different nZVI dosages.

content was produced shortly after the nZVI pulse was added to the reactor (in the range of hours), as shown in the inset of Fig. 2a. Previous work has reported that more than 90% of the total H<sub>2</sub> volume delivered by nZVI was produced in the first hour, regardless of initial nZVI concentration [43]. The same authors described that nZVI is easily deactivated during the dissolution process because of the formation of iron-related precipitates on its surface, due to its strong reducing power, resulting in much slower H<sub>2</sub> production rates after the first hour of dissolution.

During Phase 2, when the weekly dosage was split into two pulses per week, the peaks were of less magnitude, but the average value was maintained (Table 2). With the nZVI pulses suppression, in Phase 3, the methane content in biogas showed a sustained decrease, returning to values that were similar to phase 0. This behaviour shows that the nZVI accumulated in the reactor in the previous phases has a delayed background effect on the operation. Previous studies have shown the long-lasting effect of nZVI, since depending on the degree of crystallinity of the particles, complete oxidation of Fe(0) could last between two weeks and a year [44,45]. Indeed, Fe concentration evaluation during Phase 3 (Figure S2) showed that 0.45 mg<sub>Fe</sub> g<sup>-1</sup> were still present in the effluent 10 days after the last nZVI pulse. The effluent and reactor content Fe concentration decreased to 0.05 mg<sub>Fe</sub> g<sup>-1</sup> 65 days after the last pulse, following the biogas methane content decreasing tendency during Phase 3. The fate of nZVI after being corroded to Fe<sup>2+</sup> in the anaerobic digester is probably the formation of insoluble siderite (FeCO<sub>3</sub>), by interaction with CO<sub>2</sub>; or the precipitation with PO<sub>4</sub><sup>3-</sup> to form vivianite (Fe<sub>3</sub>(PO<sub>4</sub>)<sub>2</sub>), as described in both cases by Puyol and co-workers (2018) [46].

The average methane production rate increased 165% during the nZVI application phases, from 65 ± 22 to 172 ± 56 L<sub>methane</sub> kg<sub>VS</sub><sup>-1</sup> d<sup>-1</sup> (Table 2, Figure S3). Finally, no significant statistical differences were found in the COD removal efficiency in any operational phase, which presented averages in a range between 31% and 50% (Table 2). Since no significant increase in COD removal efficiency was observed, the increase in methane production may be due to hydrogenotrophic methanogens H<sub>2</sub> (produced by nZVI corrosion) uptake and reaction with CO<sub>2</sub>.

### 3.2.2. Mesophilic temperature range operation

Regarding the mesophilic reactors, a clear increase in methane content in biogas of M reactor compared to control (MC) was produced in Phase 1 (Fig. 2b). Values of 88% were reached in M reactor, while methane content in MC was in a range of 67–69%. As in the thermophilic reactor, the increase of methane content was produced some hours after the pulse and was followed by a decrease at the end of the week.

When nZVI was added also to CM reactor (Phase 2), the methane content of biogas increased and reached the values obtained in the M reactor, over 80% during the peak. On the other hand, reactor M showed a more stable methane content value when the dosage was divided into two pulses a week (Fig. 2b).

In Phase 3, methane content percentages started to decrease in both reactors in a steady way, as described for the thermophilic reactor. Fe concentration in mesophilic reactors during Phase 3 (Figure S2) showed higher values compared to T reactor, since the HRT was double than in T reactor. Fe concentration was the highest in M reactor, maybe due to differences in mixing efficiency compared to CM reactor. The effluent of M and CM reactors contained 1.5 and 0.9 mg<sub>Fe</sub> g<sup>-1</sup>, respectively, 10 days after the last pulse, which decreased to 0.48 and 0.18 mg<sub>Fe</sub> g<sup>-1</sup> on day 65. Fe concentration in the effluent in Phase 3 correlates well with the slightly higher methane content of M reactor compared to CM reactor, and the faster decrease observed in T reactor.

The methane production rate average values in Table 2 show that reactor M produced 20% more methane during Phase 1 than reactor CM, with a total increase of 94% in Phase 2. The methane production of both reactors was similar in Phase 2, when CM reactor was submitted to nZVI addition, with a 94% improvement in the CM reactor (Figure S2). The COD removal efficiencies were similar in both reactors in all the phases, as shown in Table 2, similar to the behaviour described for the thermophilic reactor.

### 3.2.3. Other operation parameters evolution

Regarding other control parameters, data corresponding to pH, alkalinity and VFA is presented as Supporting Information. pH of the 3 reactors oscillated in general between 8.0 and 8.5

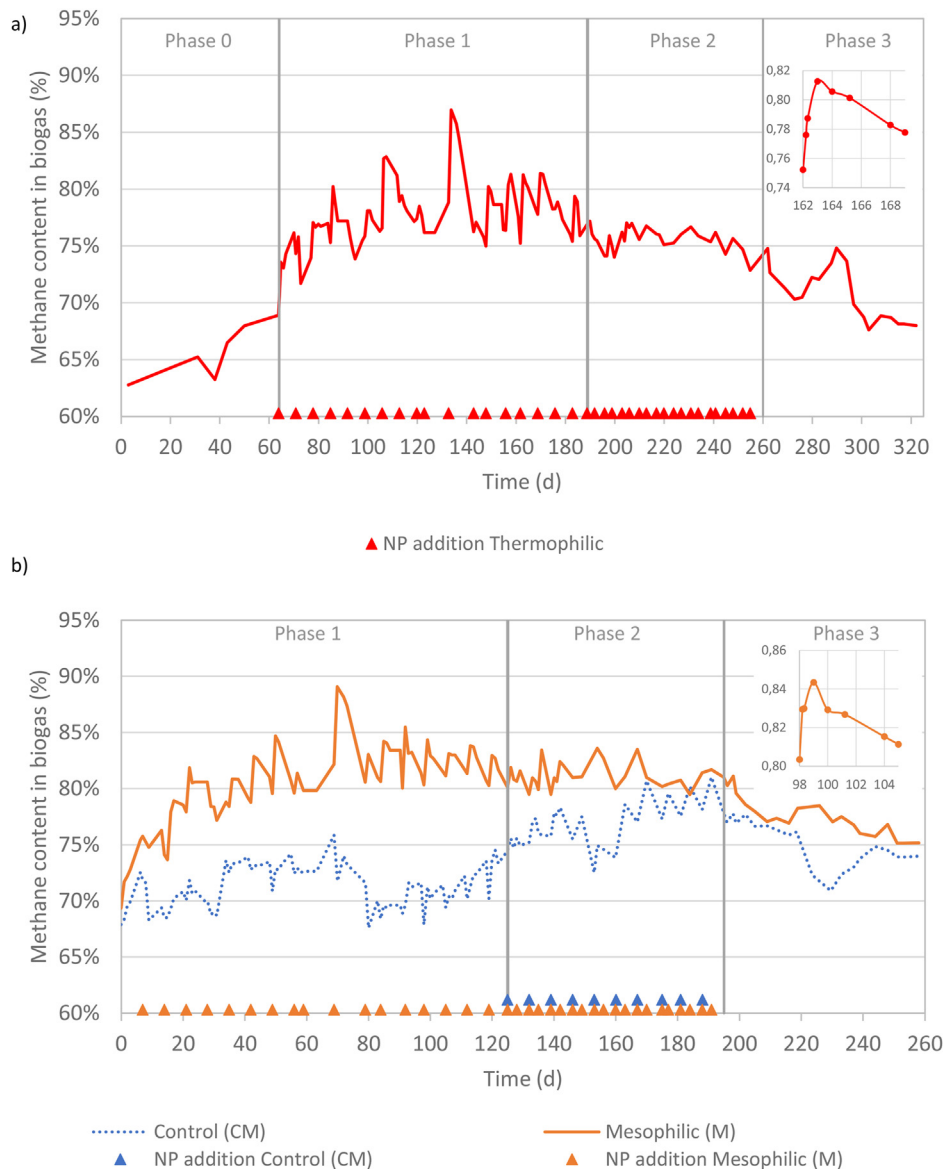


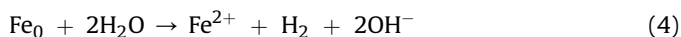
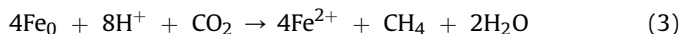
Fig. 2. Methane content in biogas in the different phases of operation in a) thermophilic temperature conditions in reactor T (detail in the inset of the peak from day 162–169); b) mesophilic temperature conditions in reactors CM and M (detail in the inset of the peak of M reactor from day 98–105).

Table 2  
Main operational results of the three reactors, mesophilic control (MC), mesophilic (M) and thermophilic (T) in the different phases (mean ± standard deviation).

| Phase | Reactor | Methane content in biogas (%) | Methane production (L kg <sub>VS</sub> <sup>-1</sup> d <sup>-1</sup> ) | COD removal (%) | pH        | Total Alkalinity (g CaCO <sub>3</sub> L <sup>-1</sup> ) | Partial Alkalinity (g CaCO <sub>3</sub> L <sup>-1</sup> ) |
|-------|---------|-------------------------------|--|-----------------|-----------|---|---|
| 1     | CM      | 71 ± 2                        | 214 ± 78   | 50 ± 9          | 8.1 ± 0.2 | 7.2 ± 0.8   | 6.5 ± 0.9   |
| 2     | CM      | 77 ± 2                        | 404 ± 100  | 46 ± 11         | 8.2 ± 0.1 | 10.7 ± 1.4  | 9.4 ± 1.3   |
| 3     | CM      | 75 ± 2                        | 342 ± 88   | 49 ± 11         | 8.3 ± 0.1 | 11.1 ± 1.0  | 9.8 ± 0.7   |
| 1     | M       | 81 ± 4                        | 255 ± 85   | 48 ± 10         | 8.3 ± 0.1 | 7.6 ± 1.2   | 6.7 ± 1.0   |
| 2     | M       | 81 ± 1                        | 402 ± 128  | 45 ± 12         | 8.5 ± 0.3 | 10.3 ± 1.2  | 8.8 ± 1.1   |
| 3     | M       | 78 ± 2                        | 321 ± 118  | 52 ± 15         | 8.4 ± 0.1 | 10.8 ± 0.7  | 9.9 ± 0.6   |
| 0     | T       | 66 ± 2                        | 65 ± 22  | 31 ± 10         | 8.2 ± 0.1 | 9.2 ± 0.9   | 7.6 ± 0.8   |
| 1     | T       | 78 ± 3                        | 140 ± 57   | 40 ± 10         | 8.2 ± 0.2 | 6.4 ± 0.7   | 5.6 ± 0.6   |
| 2     | T       | 76 ± 1                        | 172 ± 56   | 45 ± 13         | 8.4 ± 0.1 | 9.7 ± 1.0   | 7.7 ± 1.0   |
| 3     | T       | 71 ± 2                        | 146 ± 54   | 50 ± 9          | 8.2 ± 0.1 | 9.1 ± 1.2   | 7.7 ± 0.9   |

(Figure S4a and Figure S5a). Other authors have reported inhibition of the AD process at pH over 8.0 [47,48], but in this study, reactors performed in a stable way in all the operation time. An increase in pH has been reported due to the consumption of

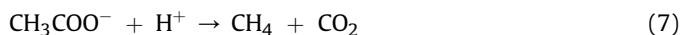
bicarbonate by hydrogenotrophic methanogens [48]. Previous research articles have reported that pH may increase or remain stable with the addition of nZVI, according to Equations (3) and (4) [22,49].



In this study, no significant statistical differences have been observed comparing CM and M reactor pH or the different operation phases (Table 2). Regarding TA and PA, all reactors showed an increase in Phase 2 (Figure S4b and Figure S5b-c), that can be related to the increase in VFA of the influent in this phase (Figure S4c-d and Figure S6). This increase in the VFA content of the influent may also explain the temporal accumulation of acetic and propionic acid in this phase, rather than being produced by methanogens inhibition.

### 3.2.4. Influence of AD operation mode on nZVI effect

The observed improvement in methane production in continuous operation mode may be due to different nZVI effects. On the one hand, the release of hydrogen during nZVI corrosion/oxidation (Equation (3)) can serve as the electron donor for methanogens [13,50], activating hydrogenotrophic metabolic pathway (Equation (5)); and homoacetogens, for the production of acetic acid (Equation (6)), which in turn could be converted into methane by acetoclastic methanogens (Equation (7)) [51].



On the other hand, nZVI may facilitate electron conduction. Several studies have shown that iron nanoparticles can accelerate direct interspecies electron transfer (DIET) [52] between bacteria and methanogens [53]. Other relative larger conductive materials that have been tested in AD, such as biochar [54] or granular activated carbon [55,56] may be used by syntrophic microorganisms as an attaching surface. Differently, NPs attach to conductive pili, reducing the requirement of multi-heme c-type cytochromes for DIET [53].

The activity stimulation of key enzymes related to hydrolysis and acidogenesis has been reported in the AD of waste activated sludge (WAS) [57]. Hydrolysis of organic compounds to soluble substances is the rate-limiting step of AD when complex particulate organic matter predominates in the substrate.

Finally, nZVI may also react with toxic substances in the reactor, such as ammonia nitrogen [5,41] or hydrogen sulphide ( $\text{H}_2\text{S}$ ) [24], lowering their concentration and alleviating inhibition phenomena on acetogens and methanogens.

The different behaviour of anaerobic digestion process observed in batch and continuous assays in this study may be due to an excess concentration of nZVI in relation to the total volume of the vial and reactors. The applied dosage was related to the amount of VSS that were added with the feeding. In the case of the continuous operation, each weekly pulse contributed to 0.6–0.7  $\text{g}_{\text{NP}} \text{L}^{-1}$  with respect to the total volume of the reactor at the moment of application, which is in the range of the higher dose tested in batch assays. But, if this amount was distributed along the week, it would correspond to a concentration of 86–103  $\text{mg}_{\text{NP}} \text{L}^{-1}$ . These values are in the range of the successful concentrations used in the studies referenced in the batch assays section.

Furthermore, in batch assays, the released  $\text{H}_2$  by corrosion of nZVI could accumulate in the headspace due to rapid nZVI dilution and produce inhibition, accompanied by reductive decomposition of cell membrane [43]. Furthermore, the possible increase of pH described in Equation (3) or a possible accumulation of VFA due to

the improvement of hydrolysis step [57] may have adversely impacted methanogenesis in batch operation, while fresh substrate addition may have helped to alleviate this effect in continuous operation [58].

### 3.3. Specific methanogenic activity

SMA of the biomass of the three reactors were determined at the end of Phase 1 and Phase 2, besides Phase 0 in T reactor (Table 3, Figure S3). M reactor showed lower SMA values for all substrates than CM reactor, except for  $\text{SMA}_{\text{H}_2}$  in Phase 2. SMA values of CM reactor also decreased in Phase 2, when nZVI was added. Using the VFA mix as a substrate decreased the SMA in comparison to the acetic acid substrate in mesophilic temperature conditions in both reactors. This reduction may be due to an inhibition of propionate or butyrate degrading bacteria. No inhibition of the acetoclastic methanogenesis metabolic pathway has been detected, corroborating the fact that the accumulation of acetic acid during Phase 2 was not due to acetoclastic methanogens inhibition.

Regarding T reactor, it showed a higher SMA value with  $\text{H}_2$  substrate than the one obtained for mesophilic reactors, which suggests better acclimatisation. The addition of nZVI boosted SMA with acetic acid and  $\text{H}_2$  substrates, which produced a 2-times increase from Phase 1 to Phase 2 and a 3-times increase from Phase 0 to Phase 1, respectively. On the contrary, the VFA mix SMA was reduced 36% from Phase 0 to Phase 2. The activation of the hydrogenotrophic metabolic pathway correlates well with methanogens using hydrogen released during nZVI corrosion/oxidation as an electron donor.

Although the evolution of the  $\text{SMA}_{\text{H}_2}$  in T reactor correlates well with the improvement shown in continuous operation, and the possibility that  $\text{H}_2$  production by nZVI corrosion may enhance hydrogenotrophic metabolic pathway, the results obtained in M reactor compared to CM reactor are not so conclusive. As it has been shown by the results of the continuous assays, the effect of nZVI addition on methane production is especially remarkable a few hours after the pulse. Therefore, once the pulses were suppressed in Phase 3, the system returned slowly to the initial values. Furthermore, Fe oxidation may accelerate once the inoculum is exposed to air for assay preparation. Therefore, the effect of nZVI on biomass may have diluted during the SMA assays.

### 3.4. Morphologic and microstructural characterization of nZVI

The SEM images obtained for the morphological characterization of nZVI showed the typical aggregation that occurs due to the existence of van der Waals forces [59] (Fig. 3a). The size of the observed particles, which describe spherical formations, were between 10 and 20 nm in diameter (Fig. 3a). This aggregation was observed in TEM with a worm-like shape (Fig. 3b). These

**Table 3**  
Specific methanogenic activity (SMA) at the start of the assay (Phase 0), and end of Phase 1 and Phase 2 of the biomass of mesophilic control (MC), mesophilic (M) and thermophilic (T) fed with different substrates. ND: not determined.

| Phase | Reactor | SMA ( $\text{mg COD}_{\text{CH}_4} \text{g}_{\text{VSS}}^{-1} \text{day}^{-1}$ ) |         |              |       |
|-------|---------|--|---------|--------------|-------|
|       |         | VFA mix  | Acetate | $\text{H}_2$ | Blank |
| 1     | CM      | 198  | 281     | 22           | 1     |
| 2     |         | 156  | 210     | 16           | 1     |
| 1     | M       | 111  | 239     | 11           | 2     |
| 2     |         | 71   | 209     | 22           | 4     |
| 0     | T       | 189  | ND      | 27           | 6     |
| 1     |         | 193  | 103     | 83           | 2     |
| 2     |         | 120  | 218     | 71           | 3     |

formations for the nZVI observed with TEM are widely described in the literature [60]. It is clearly observed, as well, how once the oxidation process of NPs begins, a needle configuration on the outside is formed, configuring a rough morphology of these as observed in Fig. 3c, which may be due to the formation of iron oxides and oxohydroxides [61]. These formations can also be seen in TEM images (Fig. 3d and e), as mentioned in the next section on oxidation of Fe NPs. TEM images also showed the contact between nZVI and bacteria present in the reactors (Fig. 3f).

A high resolution TEM image (Fig. 3g) and an electron diffraction image of selected areas (SAED) (Fig. 3h) revealed the existence of iron microcrystals with crystalline planes belonging to phases existing in the sample like the  $\alpha$  phase of iron, and other iron oxides phases. It is very likely to have iron oxohydroxides of the FeOOH type, which cannot be identified with this technique due to their amorphous nature. All the analysed images presented a typical interplanar distance of the  $\alpha$ -Fe of about 0.21 nm [62]. Other typical interplane distances of some iron oxides such as 0.14 nm and 0.25 nm [61] can be observed as well, which indicates that a part of the analysed samples presents a certain degree of oxidation, and therefore the coexistence of oxidized and unoxidized Fe. This fact coincides with the hypotheses raised in the literature [62], which state that oxidized and unoxidized areas coexist, and oxidation occurs in the external parts of the nanoparticle, as confirmed in the next section of this work. The plane distances found in all the samples analysed are very similar, with very little variability among them.

### 3.5. Oxidation state evolution of nZVI

The evolution of the oxidation states of nZVI over the days based on the information on the  $L_{32}$  index can be seen in Table 4. The time scale observed in Table 4 starts when nZVI is added to the bottle containing water (test 1a), anaerobic medium (test 1b), or to the continuous reactors (tests 2a, b), and day 1 means that the sample is taken 24 h later. As seen, within the experimental variability, the oxidation state of nZVI in test 1a) is maintained up to 14 days at  $L_{32}$  values of around 4, which corresponds to a +2 oxidation state of iron. Right after synthesis, nZVI is a little oxidized, but  $L_{32}$  ratio (3.3) is

near theoretical 2.99 corresponding to a zerovalent oxidation state. It can be stated that from the first day after the synthesis, particles increase their oxidation state to +2. However, the  $L_{32}$  ratio does not go beyond 4.2 after 14 days of the synthesis, which corresponds to an oxidation state between +2 and +3. This fact contrasts with the oxidation state evolution observed when nZVI is added to anaerobic medium both in tests 1b) and 2a, b), which entails an immediate oxidation to a +3 state, a level that was not reached even after 14 days when nZVI is in an aqueous suspension. In fact, only 10 min were necessary to reach that level of oxidation, which indicates that this process happens very quickly once nZVI comes into contact with anaerobic medium. The three tests (1b, 2a, 2b) performed including nZVI and anaerobic medium show very similar behaviour in terms of oxidation state evolution, with slightly faster oxidation for real reactors, even a little faster in the case of the thermophilic reactor, agreeing with the fact that higher temperatures normally accelerate reactions. Besides,  $L_{32}$  ratio indicates a +3 oxidation state is reached immediately, and it does not stop growing during the development of the test, which indicates that nZVI has oxidation capacity beyond +3, which agrees with the statement mentioned in section 3.2.1 about the long-lasting oxidation of nZVI.

Regarding the effects of oxidation state on morphology, two differentiated areas can be observed in all samples, one with spherical iron NPs (Fig. 3a) that are normally linked with worm-like shapes observed in TEM images, as already mentioned in the previous section (Fig. 3c), and another area of needle-shaped material, which usually corresponds to species of iron oxides and oxohydroxides (e.g.  $\text{FeCO}_3$ ,  $\text{Fe}_3\text{O}_4$ ,  $\text{Fe}_2\text{O}_3$ ,  $\text{Fe}(\text{OH})_3$  and  $\text{FeOOH}$ ) [61], which is confirmed by the fact that these latter areas are always more oxidized than the others when analysing their  $L_{32}$  index. These two areas normally coexist, as observed in Fig. 3d. It is also observed that the areas of needles are more numerous as the test progresses and that their degree of oxidation increases quite consistently throughout the days. Thus, needle shapes are scarcely observed in samples of freshly synthesized NPs, but their presence increases as the tests proceed. In addition, the images reveal that nZVI oxidation starts at the surface of the nanoparticles, which causes their hairy appearance as the oxidation proceeds (Fig. 3e).

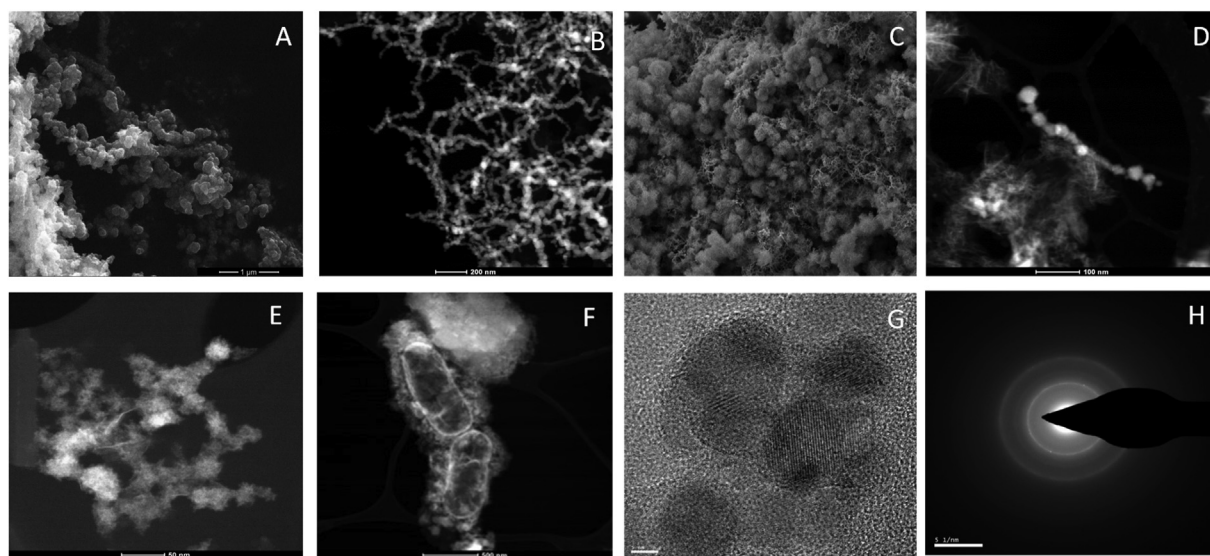


**Fig. 3.** SEM images of: a) freshly synthesized nZVI, c) nZVI one day after synthesis; TEM images of: b) freshly synthesized nZVI, d) nZVI one day after synthesis, e) nZVI from a thermophilic reactor 10 min after addition, f) nZVI-bacteria contact in a nitrogenized bottle (test 2), in the 6th day after addition, g) high resolution image of freshly synthesized nZVI, h) SAED pattern of freshly synthesized nZVI.

**Table 4**  
L<sub>32</sub> ratio data used for the evaluation of the oxidation state of nZVI in several tests up to 14 days.

| Oxidation State Evaluation Test | Day                   |          |     |     |     |     |     |     |
|---------------------------------|-----------------------|----------|-----|-----|-----|-----|-----|-----|
|                                 | 0–10 min <sup>a</sup> | 0–60 min | 1   | 2   | 3   | 6   | 7   | 14  |
| 1a) nZVI                        | 3.3                   | –        | 4.0 | 3.7 | 4.0 | 3.4 | 4.2 | 4.0 |
| 1b) nZVI + Substrate            | 4.5                   | 4.7      | 4.7 | 5.2 | 5.4 | 6.0 | 6.7 | –   |
| 2a) Mesophilic Reactor          | 4.8                   | –        | 5.2 | –   | 5.7 | –   | –   | –   |
| 2b) Thermophilic Reactor        | 4.7                   | –        | 5.4 | –   | 5.9 | –   | –   | –   |

<sup>a</sup> EELS Spectra in test 1a was only evaluated 10 min after synthesis, time scale for tests 1b, 2a and 2b starts at the moment nZVI is added to an anaerobic medium.

### 3.6. Evaluation of anaerobic digestion with nZVI addition

Although previous works have shown an improvement of methane yield with the addition of nZVI in batch AD of livestock manure, as described in section 3.1, to the authors' knowledge no continuous long-term operation assays have been reported. Different substrates have been used in previous studies in continuous operation. However, the specific characteristics of each substrate, such as pH, TS/VS, alkalinity or ammonia content, may change the effect of nZVI addition [22]. Furthermore, in those studies ZVI is used in different formats, such as scrap or iron powder. As particle size decreases, the surface-to-volume ratio increases, probably changing the properties of the material [63].

Previous studies in semi-continuous mode mesophilic AD of sewage sludge have reported an increase in methane content in biogas from 65.1% to 75.9% when dosing of 0.81 g L<sup>-1</sup> nZVI every seven days [34]. An increase from 60 to 75% was achieved by digestion of palm oil mill effluent with 16 g L<sup>-1</sup> ZVI powder addition under mesophilic conditions [58].

Compared to other in-situ biological upgrading techniques applied to livestock manure, such as H<sub>2</sub> external addition, the final methane content in biogas in this study is above the results reported in other works. For example, Luo and co-workers (2012) reported 65% methane content when digesting cattle manure with direct addition of H<sub>2</sub> to the reactor [48], while Luo and Angelidaki (2013) reported 75% methane content when co-digesting cattle manure and whey in thermophilic conditions with the same biogas upgrading technique [47].

### 3.7. Economic and environmental challenges for nZVI addition to AD

The results obtained in this study show an improvement of methane production in continuous long-term anaerobic digestion operation. The achieved biogas methane content is near the values required for methane injection in the natural gas net. In this sense, an adjustment of nZVI dosages is needed in order to determine if natural gas quality grade can be achieved, in order to avoid further upgrading steps. This partial CO<sub>2</sub> conversion in the biogas would decrease upgrading costs if methane content needed further increase. In a moment when great efforts are being made to upgrade biogas according to its methane content, this strategy supposes a clear decrease in the environmental and economic impact of these processes. Furthermore, by nZVI addition method, the total methane mass is increased, differently to other physical or chemical biogas upgrading technologies based on CO<sub>2</sub> removal. Furthermore, such as other biological technologies, the process is performed at mild operational conditions, at moderate temperature levels and atmospheric pressure, contributing to the sustainability of the technique [1].

However, up to now in-situ nZVI addition to AD is not competitive compared to established biogas upgrading techniques. nZVI production methods must ensure the efficiency of the

obtained NPs and be able to produce them at a large scale while maintaining the reproducibility in size and chemical composition. The critical point for nZVI production is the cost of NaBH<sub>4</sub>. It has been reported that the cost of nZVI production was of 0.95€ g<sup>-1</sup>, where NaBH<sub>4</sub> reactant represented 85% of this cost [64]. In order to be applicable at a large scale, nZVI cost has to be decreased, i.e. by using extracts obtained from natural products, such as leaves from oak trees [64] or alternative methods such as precision milling [65]. Further process costs reduction could be achieved by using waste streams as Fe source. Iron nanoparticles have been successfully biosynthesized from water treatment sludge, so the use of commercial chemical precursors with analytical grades (e.g. FeSO<sub>4</sub>, FeNO<sub>3</sub> and FeCl<sub>2</sub>) could be avoided [18]. The evaluation of the purity of these nanoparticles should be addressed, besides their efficiency in AD application for methane enhancement.

Finally, nanoparticles use may present an environmental challenge that needs to be evaluated. Life cycle assessment (LCA) of the use of different metallic nanoparticles in anaerobic digestion of manure has been recently performed [66]. That study reported that anaerobic digestion supplemented with NP reduced greenhouse gas emissions, acidification, eutrophication, resource depletion, ozone layer depletion potential and human toxicity potential compared with no supplemented process.

## 4. Conclusions

Batch and continuous assays have been performed in order to evaluate nZVI addition to anaerobic digestion of pig slurry, both in mesophilic and thermophilic temperature ranges. Long term continuous assays have shown a clear enhancement in methane content in biogas, in addition to an increase in methane production rate, while results in batch assays were less conclusive probably due to a low acclimation of microorganisms. Methane content in biogas in continuous operation achieved 88% and 87% in mesophilic and thermophilic conditions, respectively. The average methane production rate increased 165% and 94% with respect to the control in thermophilic and mesophilic temperature range, with nZVI dosages of 42 mg g<sup>-1</sup> SSV and 84 mg g<sup>-1</sup> SSV, respectively. nZVI showed rapid oxidation when mixed with the substrate, although the oxidation process was maintained at least for one week. Compared to conventional techniques for biogas upgrading, in situ nZVI addition would represent a decrease in investment and operation costs, although the reduction of nZVI production cost must be achieved. Furthermore, CO<sub>2</sub> would be converted in CH<sub>4</sub>, instead of removed, increasing the final methane production.

### CRedit authorship contribution statement

**Miriam Cerrillo:** Conceptualization, Methodology, Formal analysis, Investigation, Visualization, Writing – original draft, Writing – review & editing. **Laura Burgos:** Conceptualization, Investigation, Formal analysis, Writing – review & editing. **Beatriz Ruiz:** Investigation, Formal analysis. **Raquel Barrena:**

Conceptualization, Methodology, Investigation, Formal analysis, Writing – review & editing. **Javier Moral-Vico**: Conceptualization, Methodology, Investigation, Formal analysis, Visualization, Writing – original draft, Writing – review & editing. **Xavier Font**: Conceptualization, Writing – review & editing. **Antoni Sánchez**: Conceptualization, Writing – review & editing. **August Bonmatí**: Conceptualization, Project administration, Supervision, Funding acquisition, Methodology, Writing – review & editing.

### Declaration of competing interest

The authors declare that they have no known competing financial interests or personal relationships that could have appeared to influence the work reported in this paper.

### Acknowledgements

This research was funded by the Spanish Ministry of Economy and Competitiveness (INIA project RTA2015-00079-C02-01). The support of the CERCA Program and of the Consolidated Research Group TERRA (ref. 2017 SGR 1290), both from the Generalitat de Catalunya, is also acknowledged.

### Appendix A. Supplementary data

Supplementary data to this article can be found online at <https://doi.org/10.1016/j.renene.2021.08.072>.

### References

- Angelidaki, L. Treu, P. Tsapekos, G. Luo, S. Campanaro, H. Wenzel, P.G. Kougias, Biogas upgrading and utilization: current status and perspectives, *Biotechnol. Adv.* 36 (2018) 452–466, <https://doi.org/10.1016/j.biotechadv.2018.01.011>.
- D. Dong, P. Aleta, X. Zhao, O.K. Choi, S. Kim, J.W. Lee, Effects of nanoscale zero valent iron (nZVI) concentration on the biochemical conversion of gaseous carbon dioxide (CO<sub>2</sub>) into methane (CH<sub>4</sub>), *Bioresour. Technol.* 275 (2019) 314–320, <https://doi.org/10.1016/j.biortech.2018.12.075>.
- M. Cerrillo, M. Vinas, A. Bonmatí, Startup of electromethanogenic microbial electrolysis cells with two different biomass inocula for biogas upgrading, *ACS Sustain. Chem. Eng.* 5 (2017) 8852–8859, <https://doi.org/10.1021/acsschemeng.7b01636>.
- M. Tabatabaei, M. Aghbashlo, E. Valijanian, H. Kazemi Shariat Panahi, A.-S. Nizami, H. Ghanavati, A. Sulaiman, S. Mirmohamadsadeghi, K. Karimi, A comprehensive review on recent biological innovations to improve biogas production, Part 2: mainstream and downstream strategies, *Renew. Energy* 146 (2020) 1392–1407, <https://doi.org/10.1016/j.renene.2019.07.047>.
- T.W.M. Amen, O. Eljamal, A.M.E. Khalil, N. Matsunaga, Wastewater degradation by iron/copper nanoparticles and the microorganism growth rate, *J. Environ. Sci.* 74 (2018) 19–31, <https://doi.org/10.1016/j.jes.2018.01.028>.
- M. Dehghani, M. Tabatabaei, M. Aghbashlo, H. Kazemi Shariat Panahi, A.-S. Nizami, A state-of-the-art review on the application of nanomaterials for enhancing biogas production, *J. Environ. Manag.* 251 (2019), 109597, <https://doi.org/10.1016/j.jenvman.2019.03.089>.
- A. Grosser, A. Grobelak, A. Rorat, P. Courtois, F. Vandenbulcke, S. Lemièrre, R. Guyoneaud, E. Attard, P. Celary, Effects of silver nanoparticles on performance of anaerobic digestion of sewage sludge and associated microbial communities, *Renew. Energy* 171 (2021) 1014–1025, <https://doi.org/10.1016/j.renene.2021.02.127>.
- M. Farghali, F.J. Andriamanohiarisoamanana, M.M. Ahmed, S. Kotb, T. Yamashiro, M. Iwasaki, K. Umetsu, Impacts of iron oxide and titanium dioxide nanoparticles on biogas production: hydrogen sulfide mitigation, process stability, and prospective challenges, *J. Environ. Manag.* 240 (2019) 160–167, <https://doi.org/10.1016/j.jenvman.2019.03.089>.
- Z. Zhang, L. Guo, Y. Wang, Y. Zhao, Z. She, M. Gao, Y. Guo, Application of iron oxide (Fe<sub>3</sub>O<sub>4</sub>) nanoparticles during the two-stage anaerobic digestion with waste sludge: impact on the biogas production and the substrate metabolism, *Renew. Energy* 146 (2020) 2724–2735, <https://doi.org/10.1016/j.renene.2019.08.078>.
- P. Ghofrani-Isfahani, H. Baniamerian, P. Tsapekos, M. Alvarado-Morales, T. Kasama, M. Shahrokhi, M. Vossoughi, I. Angelidaki, Effect of metal oxide based TiO<sub>2</sub> nanoparticles on anaerobic digestion process of lignocellulosic substrate, *Energy* 191 (2020), 116580, <https://doi.org/10.1016/j.energy.2019.116580>.
- F. Suanon, Q. Sun, D. Mama, J. Li, B. Dimon, C.P. Yu, Effect of nanoscale zero-valent iron and magnetite (Fe<sub>3</sub>O<sub>4</sub>) on the fate of metals during anaerobic digestion of sludge, *Water Res.* 88 (2016) 897–903, <https://doi.org/10.1016/j.watres.2015.11.014>.
- G.S. Aguilar-Moreno, E. Navarro-Cerón, A. Velázquez-Hernández, G. Hernández-Eugenio, M.Á. Aguilar-Méndez, T. Espinosa-Solares, Enhancing methane yield of chicken litter in anaerobic digestion using magnetite nanoparticles, *Renew. Energy* 147 (2020) 204–213, <https://doi.org/10.1016/j.renene.2019.08.111>.
- C.-S. He, P.-P. He, H.-Y. Yang, L.-L. Li, Y. Lin, Y. Mu, H.-Q. Yu, Impact of zero-valent iron nanoparticles on the activity of anaerobic granular sludge: from macroscopic to microcosmic investigation, *Water Res.* 127 (2017) 32–40, <https://doi.org/10.1016/j.watres.2017.09.061>.
- H. Mu, Y. Chen, Long-term effect of ZnO nanoparticles on waste activated sludge anaerobic digestion, *Water Res.* 45 (2011) 5612–5620, <https://doi.org/10.1016/j.watres.2011.08.022>.
- Y. Yang, J. Guo, Z. Hu, Impact of nano zero valent iron (NZVI) on methanogenic activity and population dynamics in anaerobic digestion, *Water Res.* 47 (2013) 6790–6800, <https://doi.org/10.1016/j.watres.2013.09.012>.
- J. Gonzalez-Estrella, R. Sierra-Alvarez, J.A. Field, Toxicity assessment of inorganic nanoparticles to acetoclastic and hydrogenotrophic methanogenic activity in anaerobic granular sludge, *J. Hazard Mater.* 260 (2013) 278–285, <https://doi.org/10.1016/j.jhazmat.2013.05.029>.
- R. Barrena, E. Casals, J. Colón, X. Font, A. Sánchez, V. Puentes, Evaluation of the ecotoxicity of model nanoparticles, *Chemosphere* 75 (2009) 850–857, <https://doi.org/10.1016/j.chemosphere.2009.01.078>.
- M. Yazdani, M. Ebrahimi-Nik, A. Heidari, M.H. Abbaspour-Fard, Improvement of biogas production from slaughterhouse wastewater using biosynthesized iron nanoparticles from water treatment sludge, *Renew. Energy* 135 (2019) 496–501, <https://doi.org/10.1016/j.renene.2018.12.019>.
- B. Demirel, The impacts of engineered nanomaterials (ENMs) on anaerobic digestion processes, *Process Biochem.* 51 (2016) 308–313, <https://doi.org/10.1016/j.procbio.2015.12.007>.
- Y.-J. Lee, D.-J. Lee, Impact of adding metal nanoparticles on anaerobic digestion performance – a review, *Bioresour. Technol.* 292 (2019), 121926, <https://doi.org/10.1016/j.biortech.2019.121926>.
- E. Abdelsalam, M. Samer, Y.A. Attia, M.A. Abdel-Hadi, H.E. Hassan, Y. Badr, Influence of zero valent iron nanoparticles and magnetic iron oxide nanoparticles on biogas and methane production from anaerobic digestion of manure, *Energy* 120 (2017) 842–853, <https://doi.org/10.1016/j.energy.2016.11.137>.
- K. Bensaïda, R. Eljamal, K. Eljamal, Y. Sugihara, O. Eljamal, The impact of iron bimetallic nanoparticles on bulk microbial growth in wastewater, *J. Water Process Eng.* 40 (2021), 101825, <https://doi.org/10.1016/j.jwpe.2020.101825>.
- E. Abdelsalam, M. Samer, Y.A. Attia, M.A. Abdel-Hadi, H.E. Hassan, Y. Badr, Comparison of nanoparticles effects on biogas and methane production from anaerobic digestion of cattle dung slurry, *Renew. Energy* 87 (2016) 592–598, <https://doi.org/10.1016/j.renene.2015.10.053>.
- A. Hassanein, S. Lansing, R. Tikekar, Impact of metal nanoparticles on biogas production from poultry litter, *Bioresour. Technol.* 275 (2019) 200–206, <https://doi.org/10.1016/j.biortech.2018.12.048>.
- W. Huang, F. Yang, W. Huang, Z. Lei, Z. Zhang, Enhancing hydrogenotrophic activities by zero-valent iron addition as an effective method to improve sulfadiazine removal during anaerobic digestion of swine manure, *Bioresour. Technol.* 294 (2019), 122178, <https://doi.org/10.1016/j.biortech.2019.122178>.
- T.W.M. Amen, O. Eljamal, A.M.E. Khalil, Y. Sugihara, N. Matsunaga, Methane yield enhancement by the addition of new novel of iron and copper-iron bimetallic nanoparticles, *Chem. Eng. Process. - Process Intensif.* 130 (2018) 253–261, <https://doi.org/10.1016/j.ccep.2018.06.020>.
- T. Jia, Z. Wang, H. Shan, Y. Liu, L. Gong, Effect of nanoscale zero-valent iron on sludge anaerobic digestion, *Resour. Conserv. Recycl.* 127 (2017) 190–195, <https://doi.org/10.1016/j.resconrec.2017.09.007>.
- F. Suanon, Q. Sun, M. Li, X. Cai, Y. Zhang, Y. Yan, C.-P. Yu, Application of nanoscale zero valent iron and iron powder during sludge anaerobic digestion: impact on methane yield and pharmaceutical and personal care products degradation, *J. Hazard Mater.* 321 (2017) 47–53, <https://doi.org/10.1016/j.jhazmat.2016.08.076>.
- J. Zhou, X. You, B. Niu, X. Yang, L. Gong, Y. Zhou, J. Wang, H. Zhang, Enhancement of methanogenic activity in anaerobic digestion of high solids sludge by nano zero-valent iron, *Sci. Total Environ.* 703 (2020), 135532, <https://doi.org/10.1016/j.scitotenv.2019.135532>.
- E. Kökdemir Ünşar, N.A. Perendeci, What kind of effects do Fe<sub>2</sub>O<sub>3</sub> and Al<sub>2</sub>O<sub>3</sub> nanoparticles have on anaerobic digestion, inhibition or enhancement? *Chemosphere* 211 (2018) 726–735, <https://doi.org/10.1016/j.chemosphere.2018.08.014>.
- Y. Zhang, Z. Yang, R. Xu, Y. Xiang, M. Jia, J. Hu, Y. Zheng, W. Xiong, J. Cao, Enhanced mesophilic anaerobic digestion of waste sludge with the iron nanoparticles addition and kinetic analysis, *Sci. Total Environ.* 683 (2019) 124–133, <https://doi.org/10.1016/j.scitotenv.2019.05.214>.
- Y. Zhang, Z. Yang, Y. Xiang, R. Xu, Y. Zheng, Y. Lu, M. Jia, S. Sun, J. Cao, W. Xiong, Evolutions of antibiotic resistance genes (ARGs), class I integron-integrase (intl1) and potential hosts of ARGs during sludge anaerobic digestion with the iron nanoparticles addition, *Sci. Total Environ.* 724 (2020), 138248, <https://doi.org/10.1016/j.scitotenv.2020.138248>.
- S. Choe, S.-H. Lee, Y.-Y. Chang, K.-Y. Hwang, J. Khim, Rapid reductive destruction of hazardous organic compounds by nanoscale Fe<sub>0</sub>, *Chemosphere*

- 42 (2001) 367–372, [https://doi.org/10.1016/S0045-6535\(00\)00147-8](https://doi.org/10.1016/S0045-6535(00)00147-8).
- [34] R. Barrena, M. del C. Vargas-García, G. Capell, M. Barañska, V. Puentes, J. Moral-Vico, A. Sánchez, X. Font, Sustained effect of zero-valent iron nanoparticles under semi-continuous anaerobic digestion of sewage sludge: evolution of nanoparticles and microbial community dynamics, *Sci. Total Environ.* 777 (2021), 145969, <https://doi.org/10.1016/j.scitotenv.2021.145969>.
- [35] M. Cerrillo, L. Morey, M. Viñas, A. Bonmatí, Assessment of active methanogenic archaea in a methanol-fed upflow anaerobic sludge blanket reactor, *Appl. Microbiol. Biotechnol.* 100 (2016) 10137–10146, <https://doi.org/10.1007/s00253-016-7862-4>.
- [36] APHA, *Standard Methods for the Examination of Water and Wastewater, twentieth ed.*, American Public Health Association, American Water Works Association, and Water Pollution Control Federation, Washington, D.C., 1999.
- [37] G.K. Anderson, G. Yang, Determination of bicarbonate and total volatile acid concentration in anaerobic digesters using a simple titration, *Water Environ. Res.* 64 (1992) 53–59, <https://doi.org/10.2175/WER.64.1.8>.
- [38] H. Tan, J. Verbeeck, A. Abakumov, G. Van Tendeloo, Oxidation state and chemical shift investigation in transition metal oxides by EELS, *Ultramicroscopy* 116 (2012) 24–33, <https://doi.org/10.1016/j.ultramic.2012.03.002>.
- [39] A.C. Lizama, C.C. Figueiras, A.Z. Pedreguera, J.E. Ruiz Espinoza, Enhancing the performance and stability of the anaerobic digestion of sewage sludge by zero valent iron nanoparticles dosage, *Bioresour. Technol.* 275 (2019) 352–359, <https://doi.org/10.1016/j.biortech.2018.12.086>.
- [40] D. Wu, S. Zheng, A. Ding, G. Sun, M. Yang, Performance of a zero valent iron-based anaerobic system in swine wastewater treatment, *J. Hazard Mater.* 286 (2015) 1–6, <https://doi.org/10.1016/j.jhazmat.2014.12.029>.
- [41] Y. Yang, F. Yang, W. Huang, W. Huang, F. Li, Z. Lei, Z. Zhang, Enhanced anaerobic digestion of ammonia-rich swine manure by zero-valent iron: with special focus on the enhancement effect on hydrogenotrophic methanogenesis activity, *Bioresour. Technol.* 270 (2018) 172–179, <https://doi.org/10.1016/j.biortech.2018.09.008>.
- [42] M. Cerrillo, M. Viñas, A. Bonmatí, Unravelling the active microbial community in a thermophilic anaerobic digester-microbial electrolysis cell coupled system under different conditions, *Water Res.* 110 (2017) 192–201, <https://doi.org/10.1016/j.watres.2016.12.019>.
- [43] Y.-X. Huang, J. Guo, C. Zhang, Z. Hu, Hydrogen production from the dissolution of nano zero valent iron and its effect on anaerobic digestion, *Water Res.* 88 (2016) 475–480, <https://doi.org/10.1016/j.watres.2015.10.028>.
- [44] Y. Liu, H. Choi, D. Dionysiou, G. V. Lowry, Trichloroethene hydrodechlorination in water by highly disordered monometallic nanoiron, *Chem. Mater.* 17 (2005) 5315–5322, <https://doi.org/10.1021/cm0511217>.
- [45] Y. Liu, G.V. Lowry, Effect of particle age (Fe<sub>0</sub> content) and solution pH on NZVI reactivity: H<sub>2</sub> evolution and TCE dechlorination, *Environ. Sci. Technol.* 40 (2006) 6085–6090, <https://doi.org/10.1021/es060685o>.
- [46] D. Puyol, X. Flores-Alsina, Y. Segura, R. Molina, B. Padrino, J.L.G. Fierro, K.V. Gernaey, J.A. Melero, F. Martínez, Exploring the effects of ZVI addition on resource recovery in the anaerobic digestion process, *Chem. Eng. J.* 335 (2018) 703–711, <https://doi.org/10.1016/j.cej.2017.11.029>.
- [47] G. Luo, I. Angelidaki, Co-digestion of manure and whey for in situ biogas upgrading by the addition of H<sub>2</sub>: process performance and microbial insights, *Appl. Microbiol. Biotechnol.* 97 (2013) 1373–1381, <https://doi.org/10.1007/s00253-012-4547-5>.
- [48] G. Luo, S. Johansson, K. Boe, L. Xie, Q. Zhou, I. Angelidaki, Simultaneous hydrogen utilization and in situ biogas upgrading in an anaerobic reactor, *Biotechnol. Bioeng.* 109 (2012) 1088–1094, <https://doi.org/10.1002/bit.24360>.
- [49] L. Liang, N. Korte, B. Gu, R. Puls, C. Reeter, Geochemical and microbial reactions affecting the long-term performance of in situ 'iron barriers, *Adv. Environ. Res.* 4 (2000) 273–286, [https://doi.org/10.1016/S1093-0191\(00\)00026-5](https://doi.org/10.1016/S1093-0191(00)00026-5).
- [50] K.-F. Chen, S. Li, W. Zhang, Renewable hydrogen generation by bimetallic zero valent iron nanoparticles, *Chem. Eng. J.* 170 (2011) 562–567, <https://doi.org/10.1016/j.cej.2010.12.019>.
- [51] I. Vyrides, M. Andronikou, A. Kyrianiou, A. Modic, A. Filippeti, C. Yiakoumis, C.G. Samanides, CO<sub>2</sub> conversion to CH<sub>4</sub> using Zero Valent Iron (ZVI) and anaerobic granular sludge: optimum batch conditions and microbial pathways, *J. CO<sub>2</sub> Util.* 27 (2018) 415–422, <https://doi.org/10.1016/j.jcou.2018.08.023>.
- [52] A.-E. Rotaru, P.M. Shrestha, F. Liu, M. Shrestha, D. Shrestha, M. Embree, K. Zengler, C. Wardman, K.P. Nevin, D.R. Lovley, A new model for electron flow during anaerobic digestion: direct interspecies electron transfer to *Methanosaeta* for the reduction of carbon dioxide to methane, *Energy Environ. Sci.* 7 (2014) 408–415, <https://doi.org/10.1039/C3EE42189A>.
- [53] S. Barua, B.R. Dhar, Advances towards understanding and engineering direct interspecies electron transfer in anaerobic digestion, *Bioresour. Technol.* 244 (2017) 698–707, <https://doi.org/10.1016/j.biortech.2017.08.023>.
- [54] Z. Zhao, Y. Zhang, T.L. Woodard, K.P. Nevin, D.R. Lovley, Enhancing syntrophic metabolism in up-flow anaerobic sludge blanket reactors with conductive carbon materials, *Bioresour. Technol.* 191 (2015) 140–145, <https://doi.org/10.1016/j.biortech.2015.05.007>.
- [55] Y. Dang, D.E. Holmes, Z. Zhao, T.L. Woodard, Y. Zhang, D. Sun, L.-Y. Wang, K.P. Nevin, D.R. Lovley, Enhancing anaerobic digestion of complex organic waste with carbon-based conductive materials, *Bioresour. Technol.* 220 (2016) 516–522, <https://doi.org/10.1016/j.biortech.2016.08.114>.
- [56] F. Liu, A.-E. Rotaru, P.M. Shrestha, N.S. Malvankar, K.P. Nevin, D.R. Lovley, Promoting direct interspecies electron transfer with activated carbon, *Energy Environ. Sci.* 5 (2012) 8982–8989, <https://doi.org/10.1039/C2EE22459C>.
- [57] J. Luo, L. Feng, Y. Chen, X. Li, H. Chen, N. Xiao, D. Wang, Stimulating short-chain fatty acids production from waste activated sludge by nano zero-valent iron, *J. Biotechnol.* 187 (2014) 98–105, <https://doi.org/10.1016/j.jbiotec.2014.07.444>.
- [58] V. Domrongpakkaphan, C. Phalakornkule, M. Khemkha, In-situ methane enrichment of biogas from anaerobic digestion of palm oil mill effluent by addition of zero valent iron (ZVI), *Int. J. Hydrogen Energy* (2021), <https://doi.org/10.1016/j.ijhydene.2021.03.083>.
- [59] F. He, D. Zhao, Hydrodechlorination of trichloroethene using stabilized Fe-Pd nanoparticles: reaction mechanism and effects of stabilizers, catalysts and reaction conditions, *Appl. Catal. B Environ.* 84 (2008) 533–540, <https://doi.org/10.1016/j.apcatb.2008.05.008>.
- [60] F.S. dos Santos, F.R. Lago, L. Yokoyama, F.V. Fonseca, Synthesis and characterization of zero-valent iron nanoparticles supported on SBA-15, *J. Mater. Res. Technol.* 6 (2017) 178–183, <https://doi.org/10.1016/j.jmrt.2016.11.004>.
- [61] G. Zhen, X. Lu, Y.-Y. Li, Y. Liu, Y. Zhao, Influence of zero valent scrap iron (ZVSI) supply on methane production from waste activated sludge, *Chem. Eng. J.* 263 (2015) 461–470, <https://doi.org/10.1016/j.cej.2014.11.003>.
- [62] A. Liu, W. Zhang, Fine structural features of nanoscale zero-valent iron characterized by spherical aberration corrected scanning transmission electron microscopy (Cs-STEM), *Analyst* 139 (2014) 4512–4518, <https://doi.org/10.1039/C4AN00679H>.
- [63] H. Baniamerian, P.G. Isfahani, P. Tsapekos, M. Alvarado-Morales, M. Shahrokhi, M. Vossoughi, I. Angelidaki, Application of nano-structured materials in anaerobic digestion: current status and perspectives, *Chemosphere* 229 (2019) 188–199, <https://doi.org/10.1016/j.chemosphere.2019.04.193>.
- [64] F. Martins, S. Machado, T. Albergaria, C. Delerue-Matos, LCA applied to nano scale zero valent iron synthesis, *Int. J. Life Cycle Assess.* 22 (2017) 707–714, <https://doi.org/10.1007/s11367-016-1258-7>.
- [65] S. Li, W. Yan, W. Zhang, Solvent-free production of nanoscale zero-valent iron (nZVI) with precision milling, *Green Chem.* 11 (2009) 1618–1626, <https://doi.org/10.1039/B913056J>.
- [66] O. Hijazi, E. Abdelsalam, M. Samer, Y.A. Attia, B.M.A. Amer, M.A. Amer, M. Badr, H. Bernhardt, Life cycle assessment of the use of nanomaterials in biogas production from anaerobic digestion of manure, *Renew. Energy* 148 (2020) 417–424, <https://doi.org/10.1016/j.renene.2019.10.048>.